Title

A Dynamic Hydro-Mechanical and Biochemical Model of Stomatal Conductance for C4 Photosynthesis

Journal

Plant Physiology, 175(1)

ISSN

0032-0889

Authors

Bellasio, Chandra
Quirk, Joe
Buckley, Thomas N
et al.

Publication Date

2017-09-01

DOI

10.1104/pp.17.00666

Peer reviewed

Article:
Bellasio, C., Quirk, J. orcid.org/0000-0002-0625-8323, Buckley, T.N. et al. (1 more author) (2017) A dynamic hydro-mechanical and biochemical model of stomatal conductance for C4 photosynthesis. Plant physiology, 174 (3). ISSN 0032-0889

https://doi.org/10.1104/pp.17.00666

A dynamic hydro-mechanical and biochemical model of stomatal conductance for C_4 photosynthesis

Chandra Bellasio[1, 2, 3 *], Joe Quirk[1], Thomas N. Buckley[4], and David J. Beerling[1]

[1] *Department of Animal and Plant Sciences, University of Sheffield, Sheffield, S10 2TN, UK*
[2] *Trees and Timber institute, National Research Council of Italy, 50019 Sesto Fiorentino (Florence)*
[3] *Current address: Research School of Biology, Australian National University, Acton, ACT, 2601 Australia.*
[4] *Sydney Institute of Agriculture, University of Sydney, Narrabri NSW 2390, Australia*
*Correspondence: chandra.bellasio@anu.edu.au

Abstract

C_4 plants are major grain (maize, sorghum), sugar (sugarcane) and biofuel (*Miscanthus*) producers, and contribute ~20% to global productivity. Plants lose water through stomatal pores in order to acquire CO_2 (assimilation, A), and control their carbon-for-water balance by regulating stomatal conductance (g_S). The ability to mechanistically predict g_S and A in response to atmospheric CO_2, water availability and time is critical for simulating stomatal control of plant-atmospheric carbon and water exchange under current, past or future environmental conditions. Yet, dynamic mechanistic models for g_S are lacking, especially for C_4 photosynthesis. We developed and coupled a hydro-mechanical model of stomatal behaviour with a biochemical model of C_4 photosynthesis, calibrated using gas exchange measurements in maize, and extended the coupled model with time-explicit functions to predict dynamic responses. We demonstrated the wider applicability of the model with three additional C_4 grass species in which interspecific differences in stomatal behaviour could be accounted for by fitting a single parameter. The model accurately predicted steady-state responses of g_S to light, atmospheric CO_2 and O_2, soil drying and evaporative demand, as well as dynamic responses to light intensity. Further analyses suggest the effect of variable leaf hydraulic conductance is negligible. Based on the model, we derived a set of equations suitable for incorporation in land surface models. Our model illuminates the processes underpinning stomatal control in C_4 plants and suggests the hydraulic benefits associated with fast stomatal responses of C_4 grasses may have supported the evolution of C_4 photosynthesis.

Keywords

Mechanistic model, water use efficiency, transpiration, assimilation, time, maize.

Running title

C_4 stomatal model

Introduction

C_4 photosynthesis is a variant of the conventional C_3 photosynthetic pathway and evolved in hot, open, semi-arid environments to reduce photorespiratory energy losses. Despite being the photosynthetic type of ~3 % of species, C_4 plants contribute over 20 % to Earth's net primary productivity (NPP, abbreviations listed in Table 1) (Ehleringer et al., 1997). Moreover, maize (*Zea mays,* L.), a C_4 plant of the NADP-ME subtype, is the leading grain production cereal (FAO, 2012). C_4 photosynthesis is shared between mesophyll (M) and bundle sheath (BS) cells, which are coupled to allow the operation of a biochemical CO_2-concentrating mechanism (CCM) working through an ATP-dependent carboxylation–decarboxylation cycle (Bellasio, 2017). The CCM minimizes photorespiration by increasing the CO_2 concentration in the BS (C_{BS}), where Rubisco is exclusively expressed, allowing high assimilation (A) at low rates of transpiration (E). Consequently, C_4 plants, have higher photosynthetic water-use efficiency ($WUE=A/E$) compared with C_3 plants (Ward et al., 1999; Anderson et al., 2001; Taylor et al., 2011; Cunniff et al., 2016).

Estimating fluxes of carbon and water in and out of plants is important for predicting NPP, and studying plant responses to past and future environmental change (Ostle et al., 2009; de Boer et al., 2011; Bonan et al., 2014; Paschalis et al., 2017). The pathway of CO_2 into the plant through stomatal pores is the same as that for water vapour out, and plants regulate their carbon-for-water budget by adjusting stomatal conductance (g_S). Stomata respond, not exclusively, to light, temperature, atmospheric humidity and CO_2 concentration ($[CO_2]$) and the amount of water supplied to and within leaves from the soil (Jarvis, 1976). Compared with C_3 species, C_4 photosynthesis is more sensitive to changes in g_S, leading to increased sensitivity to soil drying if plant hydraulic conductance (K_{PLANT}) is not maintained (Ghannoum, 2009; Taylor et al., 2010; Volder et al., 2010; Taylor et al., 2011; Osborne and Sack, 2012). It was recently shown that leaf hydraulic conductivity (K_{LEAF}) is a critical bottleneck in the whole-plant hydraulic pathway and that K_{LEAF} is light-dependent (Sack and Holbrook, 2006; Osborne and Sack, 2012). Because stomatal movements are sensitive to leaf water status, g_S may in turn be influenced by the dynamics of K_{LEAF} mediated by water availability at leaf level, but these effects have not been quantified. Moreover, the stomatal and non-stomatal mechanisms governing the sensitivity of C_4 photosynthesis to soil drying are not well understood and the dynamic feedbacks between soil moisture, g_S and A are largely unknown (Wand et al., 1999; Ghannoum et al., 2000; Wand et al., 2001; Ghannoum, 2009).

Leaves continuously experience light- and shade-flecks with large transient variations in incident light intensity (*PPFD*) due to changes in cloud cover, or shading by other leaves. Stomata and photosynthesis continually respond to changes in *PPFD*, but the timing of stomatal and assimilation responses is generally not synchronised, because stomatal movements can be an order of magnitude slower than photosynthetic responses (McAusland et al., 2016). This lack of coordination between

carbon gain and water loss often results in suboptimal *WUE*, and photosynthetic losses (Lawson and Blatt, 2014).

The importance of g_S at canopy, ecosystem and global scales is recognised, and models describing stomatal behaviour coupled to leaf-level biochemical photosynthesis models form a critical component of vegetation models (Ostle et al., 2009; Berry et al., 2010; Bonan et al., 2014; Beerling, 2015; Sato et al., 2015). Within vegetation models, A is often predicted for C_3 and C_4 plants using sub-models dating from the 1980s (Berry and Farquhar, 1978), which have since been updated (Yin and Struik, 2009; Yin and Struik, 2015). Photosynthesis models are generally coupled to stomatal sub-models in order to estimate g_S from environmental or internal variables. Historically, these stomatal models have been almost exclusively empirical or phenomenological, and are often calibrated under non-limiting conditions (Ball et al., 1987; Collatz et al., 1992; Leuning, 1995; Damour et al., 2010; Way et al., 2011). Empirical models may lose accuracy the further the simulated conditions deviate from those under which the models were calibrated (Way et al., 2011), and cannot provide insight into underlying physiological mechanisms (Buckley, 2017).

Alternatively, g_S may be simulated by defining the optimal trade-off between carbon gain and water use (Givnish and Vermeij, 1976; Cowan and Farquhar, 1977; Damour et al., 2010; Manzoni et al., 2013; Buckley et al., 2016; Paschalis et al., 2017). So-called optimality models have potential application beyond plant-level, but lack biophysical underpinning and assume unlimited phenotypic plasticity in response to environmental drivers, which limits their applicability in modelling plant responses to atmospheric [CO_2] and climate change (de Boer et al., 2011; Manzoni et al., 2013; Buckley and Schymanski, 2014). In contrast, mechanistic models are underpinned by the physiological mechanisms of stomatal functioning, but there are currently no such models coupled with a biochemical model of C_4 photosynthesis.

Our objectives were to address three outstanding challenges. First, to develop and extend an existing process-based framework for modelling stomatal conductance (Buckley et al., 2003; Rodriguez-Dominguez et al., 2016) to C_4 species; second, to enable the resulting model to respond to dynamic changes in *PPFD*; and third, to interrogate the model to broaden understanding of stomatal behaviour in C_4 plants. First, we coupled a hydro-mechanical model of stomatal behaviour with biochemical sub-models for enzyme-limited and light-limited C_4 photosynthesis that were re-derived for this work. Then we developed and included sub-models accounting for CO_2 diffusion through a finite mesophyll conductance, non-stomatal limitations, uneven transitions between limitations to photosynthesis, acclimation of turgor pressure, and the effects of a light-dependent induction of K_{LEAF} on gs. Finally, we introduced time-explicit functions to simulate non steady-state responses to dynamic environmental stimuli. We calibrated the model with a comprehensive gas exchange experiment in C_4 maize and on three C_4 grasses and compared it against published datasets to explore responses to soil water potential, [CO_2], evaporative demand and *PPFD*.

104

Results

Model calibration and output overview

The coupled modelling scheme is depicted in Figure 1 to highlight which quantities are used as model inputs and which are stated variables used to calculate photosynthetic and stomatal responses. We derived photosynthetic parameters using data obtained from nine sets of measurements on maize (*Zea mays* L., Table 1, see also Table S2, the full dataset is reported in Supporting Information File S2), and three to eight sets of measurements on three C_4 grasses (*Eragrostis curvula*, *Heteropogon contortus* and *Themeda triandra*, Table S3). Stomatal movements are driven by both biochemical (ATP) and hydro-mechanical forcing, the latter of which includes guard cell responses to the water status and turgor of the leaf, which are closely related to K_{PLANT} and K_{LEAF}. In the stomatal component of the model, the biochemical driver of stomatal responses is τ, a quantity related to the concentration of ATP in BS and M chloroplasts. The influence of biochemical factors relative to hydro-mechanical forcing is determined by the parameter β, while stomatal morphology is described by χ.

Below, we describe the modelled response of A, g_S, and key variables in their calculation, to environmental drivers such as light, [CO_2] and soil water potential. We show the modelled dynamic responses of A and g_S to transient changes in light intensity that represent leaf exposure to light-flecks. Finally, we discuss a theoretical scenario in which K_{LEAF} was allowed to vary in response to *PPFD* in order to mimic the activation of aquaporins occurring upon transition from dark to light.

Responses to irradiance

Simulated stomatal conductance (g_S) and CO_2 assimilation (A) both increased non-linearly with *PPFD* (Figure 2A and C). To simulate *PPFD* responses, external [CO_2], C_a was set at 400 μmol mol^{-1} and the simulations were driven by varying *PPFD* input at 150 discrete increments at which C_M was iteratively fitted each time (Figure 1). The simulations compare well with maize data taken from Bellasio et al. (2016a), (Figure 2, circles), measured under the same C_a and at eight *PPFD* levels between 30 and 1200 μmol m^{-2} s^{-1}. Although here, A was overestimated at high *PPFD*, due to a lower J_{ATPMAX} in the data of Bellasio et al. (2016a). This dataset is ideal for comparison with our model because the measurements were taken using long acclimation time (>12 min) between *PPFD* steps (and C_a steps, see below), meaning stomatal responses were likely captured at steady-state. Stomatal responses were also simulated by coupling the photosynthetic sub-model with the stomatal sub-model of Collatz et al. (1992), parameterised after Collatz et al. (1992), and shown for comparison in Figure 2C. The enzyme- and light-limited potential rates of carboxylation [$V_{C(C)}$ and $V_{C(J)}$, respectively] and the concentration of ATP in the BS chloroplasts, τ, are used to calculate g_S and A. $V_{C(C)}$ shows an initial decline with increasing *PPFD* below ~200 μmol m^{-2} s^{-1}, due to the re-fixation of respired CO_2, and remains almost constant thereafter (Figure 2E). In contrast, $V_{C(J)}$

Figure 1. Modelling approach and framework. Blue boxes show input parameters/variables. Dashed boxes encapsulate the light-limited and enzyme-limited models for C_4 photosynthesis and the purple box represents the hydro-mechanical stomatal model. Photosynthetic photon flux density (*PPFD*) and CO_2 concentration external to the leaf [C_a] are inputs to the photosynthesis models. Electron transport and ATP production rates (J_{ATP}) and [CO_2] in mesophyll (C_M) are fed into the light- and enzyme-limited models. The outputs from the photosynthesis models are used to calculate chloroplastic ATP concentration, τ. τ is used in the stomatal model along with inputs for soil water potential, Ψ_{Soil} and evaporative demand, D_S. The stomatal model also uses other set and fitted variables (e.g. π_e, $\chi\beta$, and K_{PLANT} [see Table 1]), along with τ_0, which relates to the chloroplastic ATP concentration in the dark and is calculated from g_S in the dark (g_{S0}) and D_S in the dark (D_{S0}). In the model simulations, C_M is calculated iteratively.

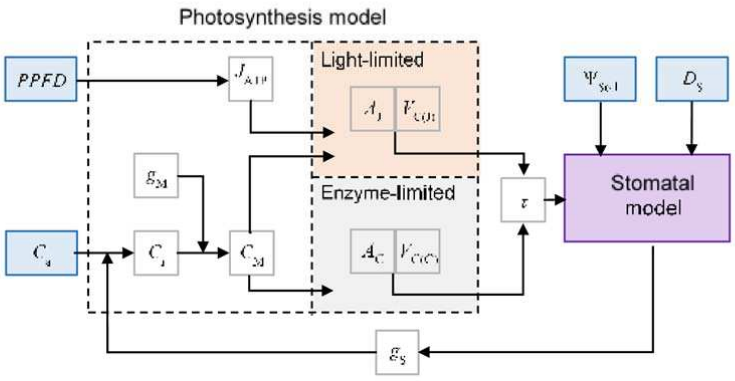

increases non-linearly with *PPFD* and has a characteristic saturating response dependent on the response of J_{ATP} to *PPFD* (Eqn 8). Because τ, in turn, depends on the ratio of $V_{C(C)}/V_{C(J)}$ (Eqn 11), it responds to increasing *PPFD* with the same saturating trend as $V_{C(J)}$. The predicted response patterns and magnitudes of A, g_S, $V_{C(C)}$, $V_{C(J)}$ and τ to increasing *PPFD* were highly conserved

Figure 2. Responses to incident irradiance (*PPFD*) of assimilation rate, *A* (**A** – **B**), stomatal conductance, g_S (**C** – **D**), and quantities underpinning the calculation of *A* and g_S (**E** – **F**) at 21% O_2 (left) and at 2% O_2 (right). The model is plotted here against data taken from Bellasio et al. (2016a) (circles, *n*=3, all data shown). The model of Collatz *et al*. (1992) is shown for comparison in Panel **C**. In Panels **E** and **F**, the bold solid line shows the ATP concentration, τ, the thin solid line the potential enzyme-limited carboxylation rate, $V_{C(C)}$, and the dashed line represents the potential light-limited carboxylation rate, $V_{C(J)}$.

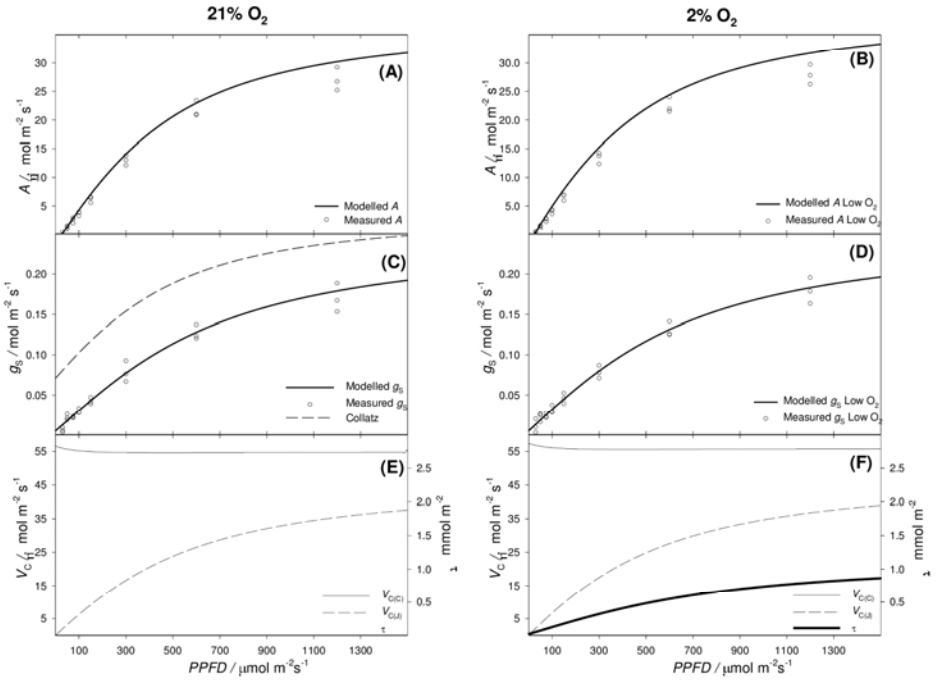

between ambient (21 %) and low (2 %) [O_2], in close agreement with data taken from Bellasio et al. (2016a) (Figure 2B, D and F). The intercellular CO_2 concentration (C_i, not shown) was initially high due to respiration, but declined to a minimum of 217 µmol mol^{-1} at a *PPFD* of 370 µmol m^{-2} s^{-1}, and thereafter followed a gradual increase with *PPFD* in line with data taken from Bellasio et al.

(2016a) and previous reports (Sharkey and Raschke, 1981). To demonstrate applicability beyond maize, the model was parameterised with photosynthetic characteristics of three additional C_4 grasses (Table S3), while interspecific differences in stomatal behaviour were described by adjusting the combined parameter χβ after (Rodriguez-Dominguez et al., 2016). The model accurately predicted A and g_S at all *PPFD*s (Figure S1).

Responses to intercellular CO_2 concentration

Simulated responses of A, g_S, $V_{C(C)}$, $V_{C(J)}$ and τ to increasing C_i (Figure 3) in maize were obtained by varying the C_a input at 89 discrete increments, and iteratively fitting C_M at each value of C_a, under a set *PPFD* of 1200 µmol m^{-2} s^{-1}. Predicted A and g_s again compared well with data from Bellasio et al. (2016a), which were measured under the same *PPFD* as the simulations (Figure 3, circles), and by setting reference [CO_2] at 9 levels between 400 and 10 µmol mol^{-1}. Simulated A increased rapidly between a C_i of 0 and 100 µmol mol^{-1}, due to the C_4 CCM, then levelled out at the *PPFD*-saturated value, while g_S initially decreased quickly as C_i approached 150 µmol mol^{-1} before continuing to decrease more gradually with increasing C_i (Figure 3A – D). Between a C_i of 0 and 50 µmol mol^{-1}, τ declined almost linearly, but the rate of decline decreased until it flattened to ~1 mmol m^{-2} at around a C_i of 150 µmol mol^{-1} (Figure 3E). As $V_{C(C)}$ surpassed $V_{C(J)}$ at a C_i of 90 µmol mol^{-1}, photosynthesis switched from enzyme-limited to light-limited, and the response of τ to C_i then decreased more rapidly before levelling out. Stomatal responses simulated with the stomatal sub-model of Collatz et al. (1992) are shown for comparison (Figure 3C). Because of the low sensitivity of C_4 photosynthesis to [O_2], both the simulated and observed responses of A, g_S, $V_{C(C)}$, $V_{C(J)}$ and τ to increasing C_i at 2% O_2 (Figure 3B, D and F) were indistinguishable from those at 21% O_2.

Responses to soil water potential

When C_4 plants experience water limitation, a portion of the overall decrease in A is driven by biochemical limitations, unrelated to stomatal movements, and is generally referred to as non-stomatal limitation (Ghannoum et al., 2003; Ghannoum, 2009). This is not accounted for by the C_4 photosynthetic model, which overestimates A at low Ψ_{Soil} (*Quirk et al.*, under review). Here, we account for non-stomatal limitations through an empirical correction (Eqn 15), which links the inputs V_{CMAX}, and J_{ATPMAX} to Ψ_{Soil} (Figure S3), preserving the ratio between J_{ATPMAX} and V_{CMAX}. Because the correction is applied to model inputs, outputs are mutually consistent and can be used for theoretical and physiological analyses. Simulated responses of A, g_S, $V_{C(C)}$, $V_{C(J)}$ and τ to increasingly negative soil water potential, Ψ_{Soil} (Figure 4) were obtained by varying Ψ_{Soil} at 257 discrete increments, and iteratively fitting C_M at each value of Ψ_{Soil}, under a set *PPFD* of 700 µmol m^{-2} s^{-1} and C_a of 400 µmol mol^{-1}. As Ψ_{Soil} started to decrease, simulated g_S declined almost linearly, driven solely by the decrease in leaf turgor. In contrast, A was initially light-limited and insensitive to g_S (Figure 4A). As Ψ_{Soil} continued to decrease, stomatal closure exerted more influence on $V_{C(C)}$,

Figure 3. Responses to intercellular CO_2 concentration, C_i of assimilation rate, A (**A – B**), stomatal conductance, g_S (**C – D**), and quantities underpinning the calculation of A and g_S (**E – F**), at 21% O_2 (left) and at 2% O_2 (right). The model (lines) is plotted here against data taken from Bellasio et al. (2016a) (circles, n=3, all data shown). The output of Collatz *et al.* (1992) is shown for comparison in Panel **C**. In Panels **E** and **F**, the bold solid line shows the ATP concentration (τ) the thin solid line the potential enzyme-limited carboxylation rate ($V_{C(C)}$), and the dashed line represents the potential light-limited carboxylation rate ($V_{C(J)}$).

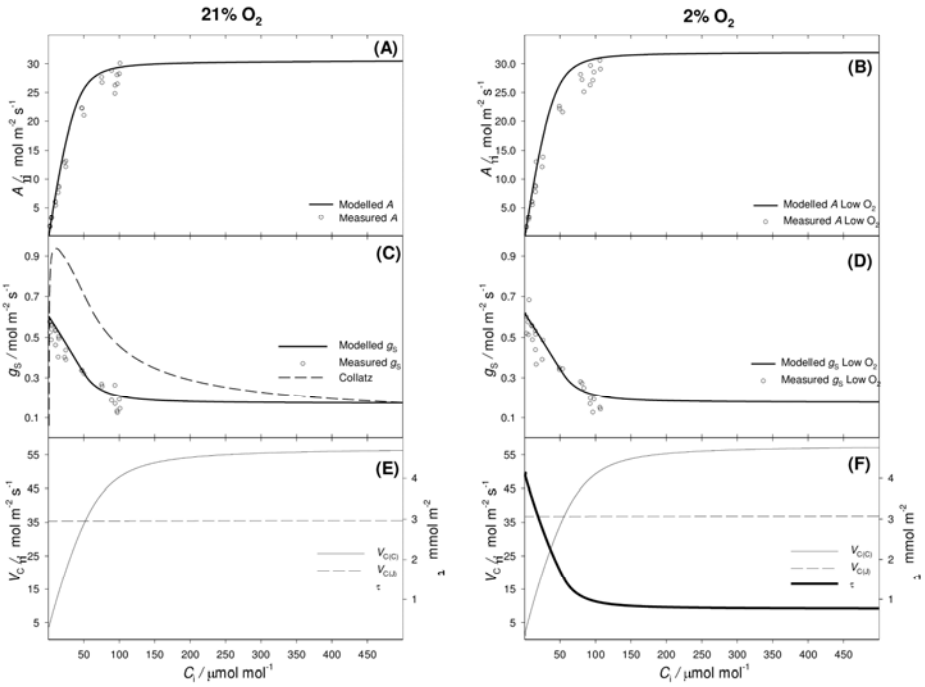

causing τ to rise sharply and the g_S response to deviate from near-linearity. When $V_{C(C)}$ declined below $V_{C(J)}$ at a Ψ_{Soil} around −1.3 MPa, A became enzyme-limited and began to decrease more rapidly with Ψ_{Soil}. As soil continued to dry the loss of guard cell turgor eventually induced stomatal

Figure 4. Responses to soil water potential, Ψ_{Soil} of assimilation rate, A (**A**), stomatal conductance, g_S (**B**), and quantities underpinning the calculation of A and g_S (**C**). The model (lines) is plotted here against independent data obtained by instantaneous gas exchange measurements on maize plants in controlled-environment growth cabinets (circles, all data shown) under a *PPFD* of 700 μmol m^{-2} s^{-1}, and reference CO_2 of 400 μmol mol^{-1}. The output of Collatz *et al*. (1992) is shown for comparison in Panel **B**. In Panel **C** the bold solid line shows the ATP concentration (τ), the thin solid line the potential enzyme-limited carboxylation rate ($V_{C(C)}$), and the dashed line represents the potential light-limited carboxylation rate ($V_{C(J)}$).

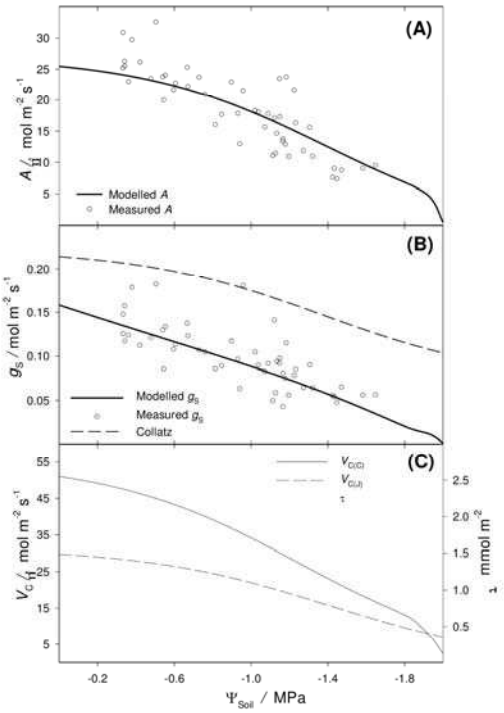

closure and g_S reached the minimal value of g_{S0} (Figure 4B). The predicted response of g_s to Ψ_{Soil} compared well with independent instantaneous measurements (Figure 4A–B, circles). There was close agreement between measured and simulated A at all values of Ψ_{Soil}. Stomatal responses

simulated with the stomatal sub-model of Collatz et al. (1992) are shown for comparison (Figure 3C).

Responses to evaporative demand (vapour pressure deficit)

The response of g_S to water vapour pressure deficit (*VPD*), represented here by the input term D_S (the water vapour mole fraction difference between the leaf and air, which is *VPD* divided by atmospheric pressure), was simulated by varying D_s and iteratively fitting C_M at each value under a set *PPFD* of 750 μmol m^{-2} s^{-1} and four levels of C_a (Figure 5A). Stomatal conductance declined hyperbolically with increasing D_S (as evaporative demand increased), with the response influenced by C_a (Figure 5). At sub-ambient [CO_2] of 200 μmol mol^{-1}, g_S was more sensitive to D_S, due to higher levels of τ which is itself induced by lower $V_{C(C)}/V_{C(J)}$ (not shown). The simulated trends were in line with the data of Morison and Gifford (1983), measured under the same *PPFD* of the simulations. However, Morison and Gifford (1983) showed a higher sensitivity of g_S to changes in *VPD*, which we partly attribute to growth differences, and partly to the fact that any feed-forward action of humidity on stomatal movement is neglected in our model (Buckley, 2005).

Dynamic responses to an increase in PPFD

Simulated dynamic responses of A and g_S to an increase in *PPFD* from 50 to 1500 μmol m^{-2} s^{-1} compared well with data for maize taken from Chen et al. (2013) (Figure 6). For the experimental measurements, maize leaves were acclimated at a *PPFD* of 50 μmol m^{-2} s^{-1} for at least 10 min before *PPFD* was increased to 1500 μmol m^{-2} s^{-1} (Chen et al., 2013). For the simulations, C_a was set at 400 μmol mol^{-1} and D_S at 10 mmol mol^{-1}, and then run with a one-second time interval, simulating the kinetics of J_{ATP} and response of g_S dynamically (Equation 16 and 17). C_M was iteratively fitted at each time point. Assimilation responded immediately to the increase in *PPFD*, but took ~10 min to reach steady state (Figure 6A). In contrast, the response of stomata was delayed relative to A, reaching steady state after ~15 min (Figure 6B–C).

Leaf hydraulic conductance

Leaf hydraulic conductance (K_{LEAF}) was found to be light-dependent in dicots (Sack and Holbrook, 2006) and maize (Kim and Steudle, 2007). The light induction is probably mediated by an increased transcription of aquaporins (Cochard et al., 2007). Here, we interrogated the model to assess whether a light-inducible K_{LEAF} would have any effect on g_S, mediated by decreased leaf water availability under low light. We described K_{LEAF} induction through a simple Michaelis-Menten saturating response, as $K_{\mathrm{LEAF}} = K_{\mathrm{LEAF\,MIN}} + \frac{PPFD(K_{\mathrm{LEAF\,MAX}} - K_{\mathrm{LEAF\,MIN}})}{PPFD + K_M(K_{\mathrm{LEAF}})}$, where $K_{LEAF\,MIN}$ is the value of K_{LEAF} in the dark, $K_{LEAF\,MAX}$ is the fully induced value of K_{LEAF} and $K_M(K_{LEAF})$ is the *PPFD* at half K_{LEAF} saturation. K_{PLANT} was calculated as $K_{\mathrm{PLANT}} = \frac{1}{\frac{1}{K_{\mathrm{STEM}}} + \frac{1}{K_{\mathrm{LEAF}}}}$. K_{STEM} was assumed

Figure 5. Modelled response of stomatal conductance, g_S to water pressure deficit, *VPD* – expressed here as mole gradient (D_S=10*VPD*) – obtained at four different CO_2 concentrations: 200 μmol mol^{-1} (thick solid line), 400 μmol mol^{-1} (dashed line), 600 μmol mol^{-1} (dotted line), 800 μmol mol^{-1} (thin solid line), under a *PPFD* of 750 μmol m^{-2} s^{-1}. Other inputs are listed in Table 1.

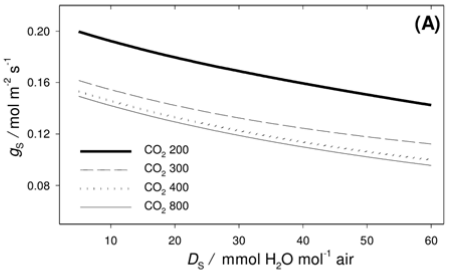

not to vary with *PPFD*, and knowing that $\frac{1}{K_{\mathrm{LEAF}}} \approx 0.3 \frac{1}{K_{\mathrm{PLANT}}}$ (Sack and Holbrook, 2006), we set a $K_{\mathrm{LEAF\ MAX}}$ of 40 mmol H_2O m^{-2} s^{-1} MPa^{-1} and a K_{STEM} of 20 mmol H_2O m^{-2} s^{-1} MPa^{-1}, so that K_{PLANT}≈12 mmol H_2O m^{-2} s^{-1} MPa^{-1} under a *PPFD* of 2000 μmol m^{-2} s^{-1}.

Figure 6. Dynamic responses of assimilation rate, A (**A**), stomatal conductance, g_S (**B**), and quantities underpinning the calculation of A and g_S (**C**) following an increase in incident light intensity, *PPFD* from 50 to 1500 μmol m^{-2} s^{-1} (vertical grey line). Modelled responses (lines) were obtained by setting g_{s0} = 0.06 mol m^{-2} s^{-1}, $\chi\beta$ = 0.39 mol air $mmol^{-1}$ ATP s^{-1} MPa^{-1}, while other inputs are listed in Table 1. The data points (circles) are taken from Chen et al. (2013) in which maize leaves were acclimated at a *PPFD* of 50 μmol m^{-2} s^{-1} for >10 min, before *PPFD* was increased to 1500 μmol m^{-2} s^{-1}. In Panel **C** the bold solid line shows the ATP concentration (τ), the thin solid line the potential enzyme-limited carboxylation rate ($V_{C(C)}$) and the dashed line represents the potential light-limited carboxylation rate ($V_{C(J)}$).

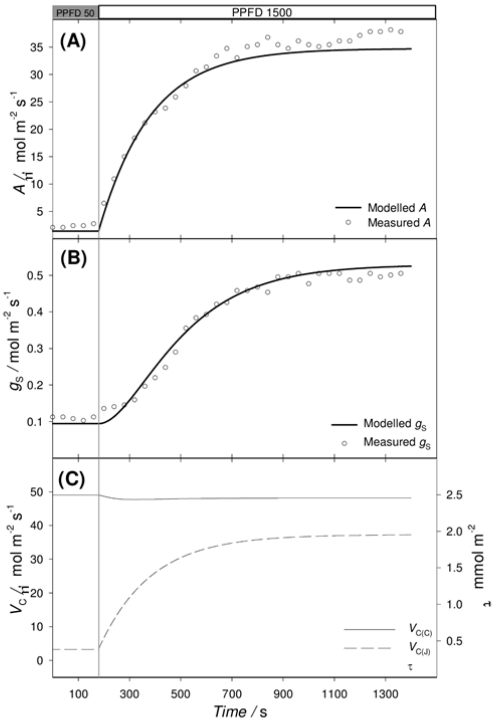

Firstly, we simulated well-watered conditions with a realistic $K_{LEAF\ MIN}$=0.5 $K_{LEAF\ MAX}$ (Sack and Holbrook, 2006). We used three different $K_M(K_{LEAF})$ (μmol m^{-2} s^{-1}): a $K_M(K_{LEAF})$=1 to represent induction in the dark, $K_M(K_{LEAF})$=200, which is the most realistic case, and $K_M(K_{LEAF})$=500 to represent induction at high *PPFD* (Figure S2). In each case, the effect on g_S was negligible (Figure

S3 A). For instance, at a *PPFD* of 200 μmol m^{-2} s^{-1}, g_S was 0.36 % and 0.6 % lower with a $K_M(K_{LEAF})$ of 200 or 500 μmol m^{-2} s^{-1} than with a $K_M(K_{LEAF})$ of 1 μmol m^{-2} s^{-1}. In a more stringent scenario we set $K_{LEAFMIN}$=0.25 $K_{LEAF\ MAX}$ (Cochard et al., 2007), again, we found that any effect on g_S was negligible (Figure S3 B). For instance at a *PPFD* of 200 μmol m^{-2} s^{-1} g_S was 0.65% and 1.2% lower with a $K_M(K_{LEAF})$ of 200 or 500 μmol m^{-2} s^{-1} than with a $K_M(K_{LEAF})$ of 1 μmol m^{-2} s^{-1}. We finally simulated an extreme case of reduced water availability (Ψ_{Soil}=−1 MPa), high evaporative demand (D_S=50 mmol H_2O mol air $^{-1}$) and $K_{LEAF\ MIN}$=0.25 $K_{LEAF\ MAX}$. Even in this case the effect on g_S was negligible (Figure S3 C). For instance, at a *PPFD* of 200 μmol m^{-2} s^{-1} g_S was 1.9% and 3.5% lower with a $K_M(K_{LEAF})$ of 200 or 500 μmol m^{-2} s^{-1} than with a $K_M(K_{LEAF})$ of 1 μmol m^{-2} s^{-1}. Overall, the outputs indicate that the light induction of K_{LEAF} does not substantially reduce g_S mediated by decreased water availability, although we cannot exclude other feedback mechanisms.

Discussion

We successfully coupled a hydro-mechanical stomatal model to a newly derived enzyme- and light-limited biochemical model of leaf-level C_4 photosynthesis calibrated for maize and demonstrated the ability of the resulting model to simulate the behaviour of three additional C_4 grass species. We establish that in maize, during a transient increase in *PPFD* (light-fleck), stomata respond after assimilation, and that slower stomatal responses to light- and shade-flecks can substantially limit the water use optimality of leaves (see dedicated paragraph below). We also show that light induction of K_{PLANT} does not reduce g_S through effects of decreased leaf-level water availability. Our model allowed accurate simulation of steady-state photosynthetic and stomatal responses to changes in *PPFD* in four C_4 species, atmospheric [CO_2], soil moisture and evaporative demand (Figures 2–5), as well as dynamic responses to light-flecks following the incorporation of time-explicit constraints on J_{ATP} and τ (Figure 6).

The hydro-mechanical and biochemical rationale underpinning the stomatal model is described fully in Buckley et al. (2003) and we followed the simplified implementation of Rodriguez-Dominguez (2016) for wider applicability. In this formulation, any turgor difference or hydraulic resistance between guard and epidermal cells is neglected and all quantities can be measured except one combined parameter, $\chi\beta$ that can be fitted. The relative simplicity of the modelling approach and the equations we have derived make them suitable for implementation in larger scale vegetation modelling.

In the stomatal model, g_S is proportional to stomatal aperture, which is in turn governed by changes in guard cell and epidermal turgor (Franks et al., 1995). The model is based on the hydroactive feedback hypothesis that passive shifts in guard cell turgor caused by changes in leaf water balance are amplified by active adjustment of guard cell osmotic pressure in proportion to leaf turgor. The ultimate result is that g_s is proportional to leaf turgor, all else being equal. This assumption is well supported by experimental evidence and apparently involves leaf-endogenous ABA synthesis [see Buckley (2017)]. Leaf turgor varies from a maximum (π_e), to zero, mediated by the equilibrium between water demand (D_S and g_S) and water supply, dependent on Ψ_{Soil} and K_{PLANT}. The latter was measured under growth conditions, under a *VPD* of ~1.7 KPa, and calculated using operational transpiration measurements made under the same conditions. Around the level of K_{PLANT} found for maize (Table 1), the model was relatively insensitive to variable K_{PLANT} (Figure S5). When K_{PLANT} was increased by 30 %, maximum g_S decreased by only ~3 %, and *vice versa*, however, the specific response to [CO_2], *PPFD*, *VPD* or Ψ_{Soil} was not affected. Furthermore, in simulations using variable K_{PLANT}, decreasing water availability under low light did not lower g_S (Figure S5). Higher sensitivities were found at lower values of K_{PLANT} (Figure S5), indicating a shift from biochemical to hydraulic control over g_S, which may occur, for instance, under water stress, where xylem cavitation causes severe dynamic declines in K_{PLANT}.

In the model, $\chi\beta$ scales the strength of the hydroactive loop to the turgor-mediated hydropassive feedback. Interspecific differences in stomatal responses between maize and three other grass species were successfully described simply by varying $\chi\beta$. In most angiosperms the hydropassive feedback has been identified as the main determinant in the regulation of stomatal conductance, mediated by hydraulic conductance (Buckley, 2005; Brodribb and McAdam, 2017). C_4 plants may have shifted their control of stomatal aperture towards a closer link with photosynthesis driven by improved water economy. This may allow tighter stomatal control, but requires increased water supply at leaf level (*Quirk et al*., under review). The resulting improvement in water relations may have constituted a key evolutionary driver of C_4 photosynthesis and even of grasses in general [see below and (Osborne and Sack, 2012; Griffiths et al., 2013)]. In fact, prior to the evolution of C_4 it is well recognised that improved plant hydraulics conferred benefits through the decrease of interveinal distance and the acquisition of a larger BS (Osborne and Sack, 2012; Griffiths et al., 2013; Bellasio and Lundgren, 2016).

Steady-state guard cell osmotic pressure is also proportional in the model to τ, a quantity related to the ATP concentration in the BS chloroplast. The quantity τ is a measure of the balance between the light and dark reactions of photosynthesis, capturing stomatal responses to factors that are thought to be mediated partly by photosynthetic processes (e.g., light and CO_2). In our model, τ is simulated empirically using a model for mesophyll chloroplastic ATP concentration originally derived for C_3 plants by Farquhar and Wong (1984). Tau is predicted through constraints on PGA reduction, RuBP regeneration and the RPP cycle (collectively, C_3 activity), which are valid in C_4 plants. Here, the C_3 activity is shared between the M and the BS chloroplasts (Bellasio and Griffiths, 2014c; Bellasio, 2017), and τ, therefore, collectively describes the energy status of the M and the BS.

Tau behaves in a manner broadly consistent with evidence suggesting that stomata respond to some measure of the poise between the supply and demand for energy carriers in photosynthesis (Wong, 1979; Messinger et al., 2006; Busch, 2014; Mott et al., 2014) – i.e., increasing with *PPFD* and decreasing with C_i. The use of τ as a predictor of stomatal behaviour is empirically based, which is justified by its capacity to predict parallel events occurring in M or BS chloroplasts, as well as in guard cells, but no direct connection is implied [for a detailed discussion see (Farquhar and Wong, 1984)]. Ultimately, the mechanism of the stomatal response is not fully understood (Buckley, 2017), and it is, therefore, not clear whether the τ model faithfully replicates the mechanistic underpinnings. For example, the τ formulation assumes that the potential capacities for ATP generation and consumption, sensed by the quantities $V_{C(J)}$ and $V_{C(C)}$, respectively, are independent of one another. Realistically, however, the actual rate of J_{ATP} will promptly respond to a decrease in C_i, mediated by an increase in non-photochemical energy dissipation, while the activity of light reactions will promptly respond to photophosphorylation levels (Kramer et al.,

2004; Foyer et al., 2012). Additionally, the τ model does not simulate responses to blue light, which are independent of photosynthesis (Shimazaki et al., 1986), nor the role of starch degradation in stomatal function (Horrer et al., 2016). Nevertheless, our results suggest that τ is a reliable predictor of stomatal behaviour in C_4 plants, as it has proved to be in many C_3 plants (Buckley et al., 2003; Diaz-Espejo et al., 2012; Rodriguez-Dominguez et al., 2016).

Response to light and shade flecks

The steady-state formulation of the model inherently precludes direct prediction of dynamic features such as the approach of stomatal conductance to a new steady-state following a change in *PPFD*. To overcome this limitation, we extended the model to simulate dynamic responses with a newly derived framework, which fused the simplicity of the approach of Vialet-Chabrand et al. (2016) with the rigour of Gross et al. (1991). The principle of this dynamic model is that J_{ATP} responds instantaneously when *PPFD* decreases, but with a delay when *PPFD* increases. Similarly, stomata will respond to any perturbation with a delay due to the kinetics of adjustment of guard cell osmotic pressure, but the time constant for that delay can differ between opening and closing movements (Lawson and Blatt, 2014). The model captures the dynamics of stomatal responses to light and CO_2 on the timescale of minutes. Although our formulation does not incorporate the transient 'wrong-way responses' (WWR) of g_s following changes in leaf water status, we note that WWR duration varies widely across species (Buckley et al., 2011), and our model may prove adequate for species with short WWRs. We did not attempt to assess this for maize. In future studies of photosynthetic efficiency at timescales shorter than one minute [e.g. (Pearcy et al., 1997)], the explicit calculation of metabolite pools, which have a central role in C_4 photosynthesis (Stitt and Zhu, 2014), will be key. Further, in our simplified day, other daytime factors, which may influence g_S dynamics, like leaf temperature and *VPD*, as well as circadian rhythms, were not accounted for.

The dynamic stomatal response following an increase in *PPFD* typically has three phases, all of which our model reliably simulated (Figure 6): an induction or lag (up to 10 min), a period of increasing g_s, and a plateau (Lawson and Blatt, 2014). Our model suggests the lag phase may result mechanistically from the lag in ATP production, in line with the conclusions of Barradas and Jones (1996). The duration of these phases and the speed of stomatal movements have important implications for NPP and *WUE*. Crops will experience light- and shade-flecks across the canopy as a result of changes in cloud cover and solar angle as well as self-shading or shading by neighbouring plants (Lawson and Blatt, 2014). Lag times reported for C_3 plants suggest that longer shade intervals may induce slower stomatal opening upon re-illumination than shorter shade intervals (Lawson and Blatt, 2014). Our model can account for the duration of shade intervals by varying the time constants for responses of both stomata and J_{ATP}. During a long shade interval, g_S will more closely approach steady-state closure, but it will also take longer to reach steady-state

upon re-illumination. Conversely, during a short-lived shade-fleck, g_S will remain further from steady-state closure, enabling stomata to re-open more quickly upon re-illumination. It is also important to note that, because the modelled stomatal response depends on τ, which is a function of J_{ATP}, the model predicts that g_S will always lag behind photosynthetic acclimation. If this prediction is correct, then perfect synchronicity between photosynthetic and g_S induction dynamics – which was identified as a desirable target for stomatal manipulation (Lawson and Blatt, 2014) – is impossible.

To illustrate the broader implications of stomatal response speed we simulated a daytime *PPFD* cycle at 10 s resolution, with ten, equally spaced 'cloud spells' of 30 min duration and *PPFD* of $1/15^{th}$ that of the 'clear sky' intensity at a given time (other inputs are given in Table 1). The time constants for stomatal responses were set at three levels that bracketed the kinetics derived for maize in this study with upper (instantaneous) and lower bounds [values derived for *Arabidopsis thaliana* (Vialet-Chabrand et al., 2016)], while the time constants for J_{ATP} responses were kept at maize physiological levels. Our calculations show that if stomata responded instantaneously to changes in *PPFD*, total carbon gain over the day would increase by 8 % (using maize g_s kinetics) or 9.2 % (using *Arabidopsis* g_s kinetics) (Figure 7 I, left), while total water loss over the day would increase by 11 % (Figure 7 J, left), reducing whole-day *WUE* by ~3 %, in both cases.

The water savings in the slow-response simulations result from the asymmetry between stomatal opening and closure. Because stomata take longer to open than close, an opening-closing cycle results in lower g_S on average compared with leaves with stomata that respond instantaneously. An alternative comparison is to investigate how stomatal response speed influences total daily carbon gain, while treating total daily water loss as a constraint imposed by the environment, and holding it equal between simulations. This requires adjusting the overall scale of g_S whilst simultaneously adjusting the time constant for *g*s responses in order to compensate for the tendency of faster-responding stomata to result in greater overall water use. We achieved this by iteratively varying the parameter χβ such that the integral of *E* over the day was equal across all simulations (Figure 7 J, right). Although these conditions result in similar daily *A* to those calculated previously (~8 % gain in *A* for instantaneous responses over both maize and *Arabidopsis* kinetic parametrisations, Figure 7 I compare left with right), the lower daily *A* obtained with delayed responses, compared with instantaneous responses, is now explained entirely by suboptimal temporal patterns of g_S.

Water use optimality

Optimality of water use is measured by the marginal carbon gain obtainable for a given marginal water loss, $\partial A/\partial E$ (the small increase in *A* that results if stomata are a little bit more open, all other conditions being equal). A pattern of g_s regulation is optimal, in the sense that it maximises total carbon gain for a given amount of water loss, if $\partial A/\partial E$ is constant over a given time interval [generally a day, but the time span and target value of $\partial A/\partial E$ are complex and debated topics, see

Figure 7. Diurnal profiles of g_S, A and the marginal carbon revenue of water use $\partial A/\partial E$ for C_4 maize. Stomatal responses were instantaneous (*fast*), with a C_4 delay derived for maize here (*delayed*), or slow (using *Arabidopsis thaliana* kinetics). Panel (**A**) shows *PPFD* over a hypothetical day, incorporating a *sin* rise to peak *PPFD* of 1800 μmol m^{-2} s^{-1} at midday and regular shading intervals corresponding to $1/15^{th}$ that of the clear sky *PPFD*. Right-hand line plots show the same curves on an expanded *x*-axis scale spanning the 90 min interval around midday. Panels show responses to *PPFD* of g_S (**C – D**), A (**E – F**), and $\partial A/\partial E$ (**G – H**), respectively. Integrated total daily A (**I**) and transpiration, E (**J**) are shown for each stomatal response speed when the day integral of E depended on stomatal speed ($\int E_{variable}$), and when $\int E$ was constrained to equal that of fast stomatal responses ($\int E_{normalised}$). $\partial A/\partial E$ was calculated by re-running the model at each time point with a 1‰ increase in g_S and all other inputs maintained from the previous run.

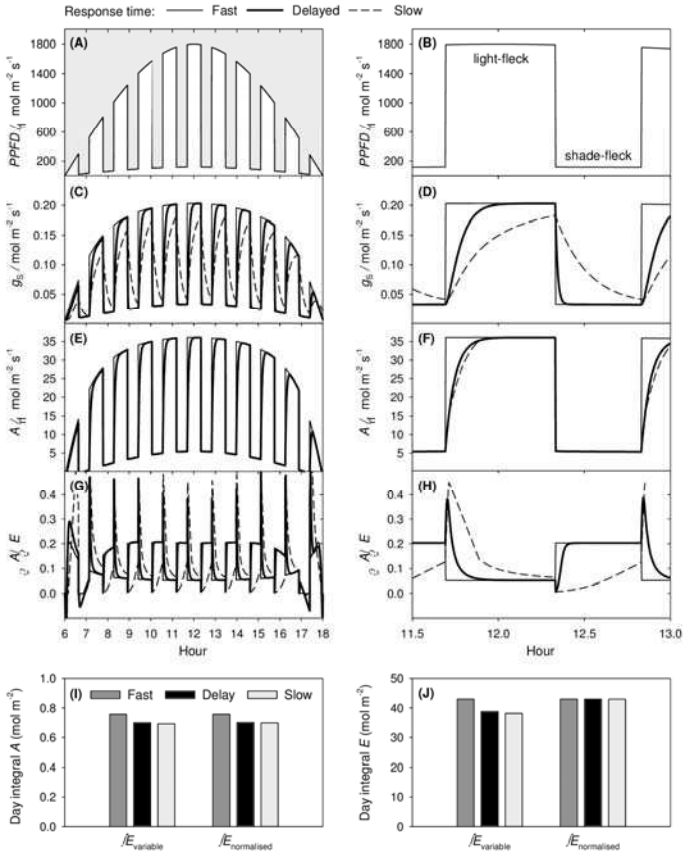

(Buckley et al., 2016)]. The same principle also applies to water allocation between parts of a plant or a canopy exposed to variable *PPFD*. Interestingly, $\partial A/\partial E$ was more variable in the delayed-response simulations than in the instantaneous-response simulations, both over the course of the day (Figure 7 G) and during a light-to-shade fleck (Figure 7 H), indicating that faster stomata were

closer to optimality. However, even where stomatal responses were instantaneous, $\partial A/\partial E$ varied between light- and shade-flecks. This indicates that the stomatal behaviour predicted by our model is suboptimal, which opens up the intriguing question of whether suboptimal water allocation is an element contributing to the poor performance of C_4 photosynthesis under low light (Sage, 2014). Further experimental work should aim to test optimality *in vivo* at the plant or field scale (Buckley et al., 2014). Further, it may be interesting to see whether C_4 plants have mechanisms to re-acclimate g_S following progressive shading by the overgrowing crop canopy, as was shown for BS conductance (Bellasio and Griffiths, 2014a, b).

We note that the improved optimality discussed above for C_4 maize was associated with a 10 times smaller time constant for stomatal opening responses than for C_3 *Arabidopsis thaliana* (Vialet-Chabrand et al., 2016). This large improvement may result in part from the dumbell-shaped guard cells of grasses, which facilitate rapid stomatal movements (Franks and Farquhar, 2007; McAusland et al., 2016), and in part from C_4 photosynthesis itself, which is generally associated with faster stomatal responses (Knapp, 1993; Franks and Farquhar, 2007; McAusland et al., 2016). We propose the association between improved hydraulics (discussed above) and faster stomatal regulation as an important, yet overlooked, driver of the evolution of grasses and C_4 photosynthesis [e.g. (Raven, 2002)]. In an evolutionary context, C_4 grasses evolved under high light and declining CO_2 in open grasslands characterised by semi-aridity (Osborne and Sack, 2012). Plants exposed to low CO_2 reduce the size of stomata, whilst increasing stomatal density (Franks et al., 2012). The integrated or net lag time of many smaller stomata to reach maximal or minimal aperture was shown to be shorter relative to fewer larger stomata (Lawson and Blatt, 2014). In this context our findings further the proposal of Osborne and Sack (2012), that C_4 photosynthesis was partly selected for and co-opted as a water-conserving mechanism, and indicate that quicker responses of stomata for C_4 plants relative to C_3 plants would confer benefits in A and $\partial A/\partial E$.

Conclusion

We developed a coupled biochemical and hydro-mechanical model of stomatal conductance for C_4 photosynthesis, and extended it with time-explicit functions allowing prediction of dynamic responses to environmental stimuli. We calibrated the C_4 model using gas exchange measurements for maize and three C_4 grass species (*Eragrostis curvula*, *Heteropogon contortus* and *Themeda triandra*), and validated it against independent datasets. We showed that following a light-fleck, stomata respond after the assimilation response, not because stomatal responses are inherently slow, but because the stomatal response is itself functionally dependent on assimilation. We also demonstrate that the slower stomata are to respond to fluctuations in light, the lower the water use optimality. We propose that fast stomatal responses, reported for maize and other C_4 grasses, may have contributed to the evolution of C_4 photosynthesis mediated by the increase of water use optimality in open, semi-arid environments. Finally, we showed that light induction of leaf

hydraulic conductance does not cause any substantial reduction in stomatal conductance mediated by decreased water availability at leaf level. Overall, the coupled model has clear promise as a predictive and analytical tool for stomatal research in C_4 species, and support (but do not prove) the hypothesis that the process framework underpinning the hydro-mechanical stomatal model remains valid for C_4 plants. The equations derived for the model are suitable for incorporation in land surface models and for detailed ecophysiological studies. Combined with the ability to predict dynamic scenarios, the model has potential for superseding the long-dominant empirical approach for stomatal modelling.

Materials and Methods

A biochemical model of C_4 photosynthesis comprising light- and enzyme-limited formulations, as well as models of CO_2 diffusion through stomata and mesophyll, was developed and coupled with a hydro-mechanical model of stomatal behaviour to yield a steady-state modelling framework – a schematic overview of which is shown in Figure 1. This framework was augmented with submodels accounting for non-stomatal limitations, uneven transition between limitations through the leaf profile, acclimation of turgor pressure under reduced water availability, and time delay functions to simulate the dynamic behaviour of stomatal responses to environmental stimuli, particularly fluctuations in light intensity.

The biochemical model of C_4 photosynthesis – enzyme-limited

To solve inconsistencies in the published equations, an enzyme-limited C_4 photosynthesis model was newly derived starting from Eqn 4.10, 4.12 and 4.16 in von Caemmerer (2000). Briefly, this formulation calculates assimilation based on CO_2 concentration at the M carboxylating sites, assuming fully activated Rubisco and PEPC, and saturating concentrations of RuBP and PEP, as:

$$A_C = \frac{-q+\sqrt{q^2-4pr}}{2p}, \quad (1)$$

where:

$$p = \frac{\alpha K_{\mathrm{C}}}{0.047 g_{BS} K_{\mathrm{O}}} - \frac{1}{g_{BS}};$$

$$q = C_{\mathrm{M}} + \frac{V_{\mathrm{P}}}{g_{BS}} - \frac{R_{\mathrm{M}}}{g_{BS}} + K_{\mathrm{C}} + \frac{O_{\mathrm{M}} K_{\mathrm{C}}}{K_{\mathrm{O}}} + \frac{R_{\mathrm{LIGHT}} \alpha K_{\mathrm{C}}}{0.047 g_{BS} K_{\mathrm{O}}} - \frac{R_{\mathrm{LIGHT}}}{g_{BS}} + \frac{V_{\mathrm{CMAX}}}{g_{BS}} + \frac{\alpha \gamma^* V_{\mathrm{CMAX}}}{0.047 g_{BS}};$$

$$r = R_{\mathrm{LIGHT}} \left(C_{\mathrm{M}} + \frac{V_{\mathrm{P}}}{g_{BS}} - \frac{R_{\mathrm{M}}}{g_{BS}} + K_{\mathrm{C}} + \frac{O_{\mathrm{M}} K_{\mathrm{C}}}{K_{\mathrm{O}}} \right) - C_{\mathrm{M}} V_{\mathrm{CMAX}} - \frac{V_{\mathrm{P}} V_{\mathrm{CMAX}}}{g_{BS}} + \frac{R_{\mathrm{M}} V_{\mathrm{CMAX}}}{g_{BS}} + \gamma^* O_{\mathrm{M}} V_{\mathrm{CMAX}}.$$

In Eqn 1, 0.047 is a coefficient scaling O_2 and CO_2 diffusivity (von Caemmerer, 2000); α is the fraction of O_2 evolution in the BS; K_C and K_O are the Rubisco Michaelis-Menten constants for CO_2 and O_2, respectively; R_M is the fraction of R_{LIGHT} in the mesophyll (0.5 R_{LIGHT}); g_{BS} is the fitted BS conductance to CO_2 diffusion; γ* is half the reciprocal of Rubisco CO_2/O_2 specificity; C_M is calculated using an M supply function, Eqn 16; O_M is the O_2 concentration in mesophyll (see Table

1 for details); V_{CMAX} is the CO_2-saturated rate of Rubisco carboxylation; and, finally V_P, the rate of PEPC carboxylation, was calculated using a Michaelis-Menten equation as:

$$V_{P(C)} = \frac{C_M V_{PMAX}}{C_M + K_P}, \quad (2)$$

where V_{PMAX} is the maximal rate of PEP carboxylation, and K_P is the PEPC Michaelis-Menten constant for HCO_3^- (Table 1). The concentration of CO_2 in the BS was estimated by mass balance of the M:

$$C_{BS(C)} = \frac{V_P - A - R_M}{g_{BS}}, \quad (3)$$

The O_2 concentration in the BS is:

$$O_{BS} = \frac{\alpha A}{0.047 g_{BS}} + O_M. \quad (4)$$

The rate of enzyme-limited Rubisco carboxylation is:

$$V_{C\,(C)} = \frac{C_{BS} V_{CMAX}}{C_{BS} + K_C\left(1 + \frac{O_{BS}}{K_O}\right)}, \quad (5)$$

and is used to calculate the Rubisco oxygenation rate:

$$V_{O\,(C)} = V_{C\,(C)}\, 2\,\gamma * \frac{O_{BS}}{C_{BS}}. \quad (6)$$

Biochemical modelling of C_4 photosynthesis – light-limited

Light-limited C_4 photosynthesis was modelled after von Caemmerer (2000). Briefly this formulation assumes that light limits assimilation, mediated by the ATP made available through photophosphorylation [for more on assumptions see (Bellasio and Griffiths, 2014a, b)]. The total ATP production rate is assumed to be entirely used by C_4 activity and C_3 activity and split between those by a parameter, called *x*, which is assumed constant at 0.4. Assimilation is:

$$A_J = \frac{-b - \sqrt{b^2 - 4ac}}{2a}, \quad (7)$$

where:

$a = 1 - \frac{7\alpha\gamma^*}{3 \cdot 0.047}$;

$b = -\left\{\frac{x J_{ATP}}{2} - R_M + g_{BS} C_M + \frac{(1-x) J_{ATP}}{3} - R_{LIGHT} + \frac{7\, g_{BS}\, \gamma^* O_M}{3} + \frac{\alpha\gamma^*}{0.047}\left(\frac{(1-x) J_{ATP}}{3} + \frac{7 R_{LIGHT}}{3}\right)\right\}$;

$c = \left(\frac{x J_{ATP}}{2} - R_M + g_{BS} C_M\right)\left(\frac{(1-x) J_{ATP}}{3} - R_{LIGHT}\right) - g_{BS}\, \gamma^* O_M \left(\frac{(1-x) J_{ATP}}{3} + \frac{7 R_{LIGHT}}{3}\right)$;

in which J_{ATP} was calculated from an empirical non-rectangular hyperbola as:

$$J_{ATP} = \frac{Y(J_{ATP})_{LL}\, PPFD + J_{ATPMAX} - \sqrt{(Y(J)_{LL}\, PPFD + J_{ATPMAX})^2 - 4\theta J_{ATPMAX} Y(J_{ATP})_{LL}\, PPFD}}{2\theta} \quad (8)$$

where, J_{ATPMAX} is the light-saturated electron transport rate, $Y(J_{ATP})_{LL}$ is the conversion efficiency of *PPFD* into J_{ATP}, and θ is an empirical factor, defining the curvature (Table 1).

Taken from Eqn 16 and 17 in Bellasio et al. (2016a), the light-limited rate of Rubisco oxygenation was solved as:

$$V_{\mathrm{O\,(J)}} = \frac{(1-x)J_{\mathrm{ATP}} - 3(A+R_{\mathrm{LIGHT}})}{5}. \quad (9)$$

$C_{\mathrm{BS\,(J)}}$ and $O_{\mathrm{BS\,(J)}}$ were calculated through Eqn 3 and 4 respectively, where $V_{\mathrm{P(J)}}=0.5xJ_{\mathrm{ATP}}$, and, finally, $V_{\mathrm{C\,(J)}}$ was calculated by inverting Eqn 6, with $V_{\mathrm{O\,(J)}}$ calculated through Eqn 9.

The hydro-mechanical model of stomatal behaviour

The hydro-mechanical model used here is a simplified formulation of the model of Buckley *et al*. (2003) following the derivation of Rodriguez-Dominguez et al. (2016). The model assumptions are described in the *Discussion*. The model calculates g_{S} as:

$$g_{\mathrm{S}} = \max\left(g_{\mathrm{S}\,0}, \frac{\chi\beta\tau(\Psi_{\mathrm{Soil}}+\pi_e)}{1+\chi\beta\tau R D_{\mathrm{S}}}\right), \quad (10)$$

where χβ is a lumped parameter scaling turgor-to-conductance and the hydro-mechanical-to-biochemical response; Ψ_{Soil} is soil water potential; π_{e} is epidermal osmotic pressure; τ is related to the ATP concentration in BS chloroplasts; R is the effective hydraulic resistance to the epidermis, calculated as $1/K_{\mathrm{PLANT}}$; and D_{S} is the leaf-to-boundary layer H_2O mole fraction gradient, a measure of vapour pressure deficit, *VPD*. The parameter τ encompasses the biochemical components of the model and is calculated from one of two values depending on the limit to photosynthesis, after Farquhar and Wong (1984), using output from the enzyme- and light-limited photosynthesis models:

$$\tau = \tau_0 + \begin{cases} \tau_C & \text{if } V_{C\,(C)} < V_{C\,(J)} \\ \tau_J & \text{else} \end{cases}. \quad (11)$$

When assimilation is enzyme-limited, $V_{\mathrm{C(C)}}<V_{\mathrm{C(J)}}$, τ_{C} is calculated as:

$$\tau_C = \alpha_t - p\frac{V_{\mathrm{C\,(C)}}}{V_{\mathrm{C\,(J)}}}, \quad (12)$$

where α_{t} is the total concentration of adenylates; and p is the concentration of photophosphorylation sites (Table 1).

When assimilation is light-limited, $V_{\mathrm{C(C)}}>V_{\mathrm{C(J)}}$, τ_{J} is:

$$\tau_{\mathrm{J}} = \frac{(\alpha_{\mathrm{t}}-p)\left(\frac{V_{\mathrm{R}}}{E_{\mathrm{T}}}-1\right)}{\frac{V_{\mathrm{C\,(C)}}}{V_{\mathrm{C\,(J)}}}\frac{V_{\mathrm{R}}}{E_{\mathrm{T}}}-1}, \quad (13)$$

where V_{R} is the potential RuBP pool size and E_{T} is the total concentration of Rubisco carboxylating sites (Table 1).

The basal level of ATP activity due to other metabolic processes including mitochondrial respiration is defined as τ_0. Here, we calculated τ_0, based on the gas exchange data, by inverting Eqn 10:

$$\tau_0 = \frac{1}{\chi\beta\left(RD_{S0} - \frac{\Psi_{Soil0}}{g_{S0}} - \frac{\pi_e}{g_{S0}}\right)}, \quad (14)$$

where g_{S0} (mol m^{-2} s^{-1}) is stomatal conductance measured in the dark; and D_{S0} is the evaporative demand measured in the dark, and Ψ_{Soil0} is the corresponding Ψ_{Soil} (here, 0 MPa).

Non-stomatal limitations

The biochemical model described above assumes that photosynthetic potential is maintained regardless of plant water status. Although, it is well-known that C_4 plants respond to decreasing Ψ_{Soil} with an overall downregulation of photosynthetic activity, through processes collectively referred to as non-stomatal limitation. These include source-sink feedbacks, reduced supply of substrates to carboxylases, limitations imposed by the diffusion of metabolites between M and BS, and a downregulation of photosynthetic potential (V_{CMAX}, V_{PMAX} and J_{ATPMAX}). Here, for simplicity we combine these limitations and describe them as a downregulation of V_{CMAX} and J_{ATPMAX} using an attenuating function from Osborne and Sack (2012):

$$Parameter = \frac{Parameter_{MAX}}{1+e^{-\frac{\Psi_{Soil}+b}{c}}}, \quad (15)$$

where $Parameter_{MAX}$ may be V_{CMAX} or J_{ATPMAX} fitted under well-watered conditions, b is the water potential when $Parameter$=0.5 $Parameter_{MAX}$, which we set to equal osmotic pressure at full watering (−1.2 MPa), while c defines the shape of the sigmoidal curve and was set at 0.5; outputs are shown in Figure S4. In the simulations where Ψ_{Soil} is constant, $Parameter$=$Parameter_{MAX}$.

Combining the submodels

The original model of von Caemmerer (2000) assumes a discrete 'jump' at the point corresponding to the transition between light-limited and enzyme-limited assimilation. Buckley et al. (2016) noted that, realistically, this transition would be smooth and occur at different C_M depending on the position of the chloroplasts through the leaf profile. Here we describe the smoothed relationship (A_{MOD}) in terms of a non-rectangular hyperbola as:

$$A_{MOD} = \frac{A_C + A_J - \sqrt{(A_C + A_J)^2 - 4\theta_A A_C A_J}}{2\theta_A}, \quad (16)$$

where θ_A was set at 0.93. A set of equations to simulate all the key photosynthetic quantities, consistent with Eqn 16, is reported in Supplementary Information Note S1.

Mesophyll CO_2 concentration, C_M, is:

$$C_M = C_i - \frac{A_{MOD}}{g_M}, \quad (17)$$

where $C_i = C_a - \frac{A_{MOD}}{g_S}$, and g_M is mesophyll conductance to CO_2 diffusion (Table1). Seed values of C_M were used to calculate Eqn 1, 2, and 7, and then iteratively fitted to Eqn 17 with g_S calculated through Eqn 10 (see Figure 1).

Dynamic stomatal responses

One important factor for stomatal dynamics has been identified as the delay to reach a steady-state stomatal aperture after a change in *PPFD* (Lawson and Blatt, 2014). Here, stomatal dynamics were accounted for by describing the time dependence of J_{ATP} and τ with a set of recursive equations analogous to Vialet-Chabrand et al. (2016):

$$\tau_t = \tau_{t-1} + \begin{cases} \frac{\tau - \tau_{t-1}}{K_i} & \text{if } \tau_{t-1} < \tau \\ \frac{\tau - \tau_{t-1}}{K_d} & \text{else} \end{cases}, \quad (18)$$

where τ_t and τ_{t-1} are the values at the time step t or at the previous step t-1; τ is the steady state value (Eqn 11), K_i and K_d are the time constants for an increase and decrease in g_S, respectively.

Similarly, we write:

$$\begin{cases} J_{ATP\,t} = J_{ATP\,t-1} + \frac{J_{ATP} - J_{ATP\,t-1}}{K_J} & \text{if } J_{ATP\,t-1} < J_{ATP} \\ J_{ATP\,t} = J_{ATP} & \text{else} \end{cases}, \quad (19)$$

where K_J is the time constant for an increase in J_{ATP}, J_{ATPt} and J_{ATPt-1} are the values at the time step t or at the previous step t-1; J_{ATP} is the steady state value (Eqn 8).

Plant growth conditions, leaf measurements and model parameterisation

Zea mays L. (F1 Hybrid PR31N27, Pioneer Hi-bred, Cremona, IT), *Eragrostis curvula*, *Heteropogon contortus* and *Themeda triandra* plants were grown in 2.5 dm^3 pots filled with three-parts commercial loam-free top soil (Boughton Ltd. Kettering, UK) plus one-part John Innes No.3 compost (John Innes Manufacturers Association, Reading, UK). Plants were grown in controlled-environment growth rooms (BDR16, Conviron Ltd, Winnipeg, Canada) with a 14-hr photoperiod of 700 (maize) or 350 (grasses) µmol m^{-2} s^{-1} *PPFD* Light was provided from a 3:1 mix of 39 W white-fluorescent tubes (Master TL5, Philips, Eindhoven, Netherlands) and 39 W red-blue fluorescent tubes (Grolux T5, Havells-Sylvania, Newhaven, UK), augmented with six 105 W halogen light bulbs (GLS, Havells-Sylvania). Air temperature was 27 °C / 18 °C (day / night) and relative humidity was 70 % / 50 % (day / night). Plants were manually watered every one-to-three days to provide variation in soil water availability over natural wetting and drying cycles.

To determine transpiration (E), assimilation (A) and g_S under operational growth conditions, instantaneous leaf gas exchange at midday was measured within the growth chambers on young, fully expanded leaves under a *PPFD* of 700 (maize) or 350 (grasses) µmol m^{-2} s^{-1}, and reference $[CO_2]$ of 400 µmol mol^{-1} with an infra-red gas analyser (IRGA, LI6400XT, LI-COR, USA), fitted

with a 6400-40 leaf chamber fluorometer for maize and a red-blue LED light source (6400-02B, LI-COR Biosciences) for the three C_4 grass species (Bellasio et al., 2016b). Leaf water potential at midday (Ψ_{MD}) and midnight (Ψ_{MN}) (a proxy for soil water potential, Ψ_{Soil}) were measured on the apical portion of fully light exposed leaves cut the day and night following instantaneous gas exchange measurements with varying time since last watering to yield measurements at a range of soil water availability. Leaf water potential was measured using a pressure chamber (PMS Instrument Company, Model 1000, Albany, USA). Plant hydraulic conductance (K_{PLANT}) was calculated as $E/(\Psi_{MN}-\Psi_{MD})$ (Fini et al., 2013).

Photosynthetic response curves (an A-C_i and A-$PPFD$ curve under ambient (21 %) and low (2 %) O_2 (maize only) were measured at the bench in a randomised order on n = 9, 8, 5 and 3 (maize, *Eragrostis Heteropogon* and *Themeda*, respectively) plants. Primary gas exchange data were corrected for CO_2 diffusion (Boesgaard et al., 2013) as:

$$A = Photo + \frac{0.4\,(400-C_a)}{100\,Area} \qquad 19$$

where *Photo* is the uncorrected assimilation as calculated by the LI-COR software, 400 is the external CO_2 concentration, C_a is the CO_2 concentration in the cuvette, and *Area* is leaf area within the cuvette: 2 cm^2 (maize) or 6 cm^2 (grasses). C_i was recalculated using A calculated with Eqn 19. Diffusion-corrected data are reported in Supporting Information File S2. Data were analysed following the 13-step protocol of Bellasio et al. (2016a) to derive a suite of photosynthetic parameters (Table 1, and Table S2).

To parameterise the model, g_{BS}, J_{ATPMAX}, R_{LIGHT}, V_{PMAX}, θ, and $Y(ATP)_{LL}$ were derived through the analysis described above (Table 1 and S3); V_{CMAX} is not well constrained by gas exchange (Pinto et al., 2014), and for maize was taken from von Caemmerer (2000), or calculated as $J_{ATPMAX}/4$ (grasses); K_C, K_O, and K_P were taken from Ubierna et al. (2016); g_M was taken from Barbour et al. (2016), O_M was assumed to equal ambient [O_2]; g_{S0} and D_{S0} were averaged from measurements taken in the dark; V_R was set at 150 mmol m^{-2} after Farquhar and Wong (1984); p and E_t were set at the values reported in Farquhar and Wong (1984); a_t was initially set at the values reported in Farquhar and Wong (1984) and then empirically adjusted (−30%) such that the output from Eqn 10 fitted observations at low C_i (Fig 3C); π_e was linked to Ψ_{Soil} through a simple linear relationship, $\pi_e = 1.2 - 0.4\,\Psi_{Soil}$, derived by liner regression of data from Sharp and Davies (1979). When responses were simulated under well-watered conditions, Ψ_{Soil} was set at 0 MPa. We derive χ and β as a single quantity, $\chi\beta$ after Rodriguez-Dominguez et al. (2016). χβ is dependent on stomatal morphology, which is in turn under environmental control (Franks and Farquhar, 2007), and we consequently expect χβ to differ between species and respond to environmental growing conditions. χβ was initially set at the values reported in Buckley et al. (2003) and then empirically adjusted such that the output from Eqn 10 fitted observations at high *PPFD* (for maize Figure 2 C, for grasses Figure S3 A, B and C). The time constants defining increases and decreases in g_S (K_i, K_d) or

591 increase in J_{ATP} (K_J) were derived through curve-fitting with the dataset reported in Figure 6. For
592 clarity and simplicity the fitting described in this paragraph was done by manual adjustment,
593 avoiding automated routines. All model parameters and values are listed in Table 1 and S3
594 (grasses).

595 **Acknowledgments**

596 We acknowledge funding through an ERC advanced grant (CDREG, 322998) awarded to DJB.
597 We thank David Johnson for technical assistance, and Davide Gusberti for maize seeds. TNB was
598 supported by the Australian Research Council (DP150103863 and LP130100183), the Grains
599 Research and Development Corporation (US00089) and the National Science Foundation (grants
600 no. 1146514 and 1557906).

601 The Authors have no conflict of interest.

602

603

604

Parsed Citations

Anderson LJ, Maherali H, Johnson HB, Polley HW, Jackson RB (2001) Gas exchange and photosynthetic acclimation over subambient to elevated CO2 in a C3-C4 grassland. Global Change Biology 7: 693-707

Pubmed: Author and Title
CrossRef: Author and Title
Google Scholar: Author Only Title Only Author and Title

Ball JT, Woodrow IE, Berry JA (1987) A model predicting stomatal conductance and its contribution to the control of photosynthesis under different environmental conditions. In J Biggins, ed, Progress in photosynthesis research: Volume 4 Proceedings of the VIIth International Congress on Photosynthesis Providence, Rhode Island, USA, August 10-15, 1986. Springer Netherlands, Dordrecht, pp 221-224

Pubmed: Author and Title
CrossRef: Author and Title
Google Scholar: Author Only Title Only Author and Title

Barbour MM, Evans JR, Simonin KA, von Caemmerer S (2016) Online CO2 and H2O oxygen isotope fractionation allows estimation of mesophyll conductance in C4 plants, and reveals that mesophyll conductance decreases as leaves age in both C4 and C3 plants. New Phytologist 210: 875-889

Pubmed: Author and Title
CrossRef: Author and Title
Google Scholar: Author Only Title Only Author and Title

Barradas VL, Jones HG (1996) Responses of CO2 assimilation to changes in irradiance: Laboratory and field data and a model for beans (Phaseolus vulgaris L.). Journal of Experimental Botany 47: 639-645

Pubmed: Author and Title
CrossRef: Author and Title
Google Scholar: Author Only Title Only Author and Title

Beerling DJ (2015) Gas valves, forests and global change: a commentary on Jarvis (1976) 'The interpretation of the variations in leaf water potential and stomatal conductance found in canopies in the field'. Philosophical Transactions of the Royal Society B: Biological Sciences 370

Pubmed: Author and Title
CrossRef: Author and Title
Google Scholar: Author Only Title Only Author and Title

Bellasio C (2017) A generalised stoichiometric model of C3, C2, C2+C4, and C4 photosynthetic metabolism. Journal of Experimental Botany 68: 269-282

Pubmed: Author and Title
CrossRef: Author and Title
Google Scholar: Author Only Title Only Author and Title

Bellasio C, Beerling DJ, Griffiths H (2016a) Deriving C4 photosynthetic parameters from combined gas exchange and chlorophyll fluorescence using an Excel tool: theory and practice. Plant, Cell & Environment 39: 1164-1179

Pubmed: Author and Title
CrossRef: Author and Title
Google Scholar: Author Only Title Only Author and Title

Bellasio C, Beerling DJ, Griffiths H (2016b) An Excel tool for deriving key photosynthetic parameters from combined gas exchange and chlorophyll fluorescence: theory and practice. Plant Cell and Environment 39: 1180-1197

Pubmed: Author and Title
CrossRef: Author and Title
Google Scholar: Author Only Title Only Author and Title

Bellasio C, Griffiths H (2014a) Acclimation of C4 metabolism to low light in mature maize leaves could limit energetic losses during progressive shading in a crop canopy. Journal of Experimental Botany 65: 3725-3736

Pubmed: Author and Title
CrossRef: Author and Title
Google Scholar: Author Only Title Only Author and Title

Bellasio C, Griffiths H (2014b) Acclimation to Low Light by C4 maize: Implications for Bundle Sheath Leakiness. Plant Cell and Environment 37: 1046-1058

Pubmed: Author and Title
CrossRef: Author and Title
Google Scholar: Author Only Title Only Author and Title

Bellasio C, Griffiths H (2014c) The operation of two decarboxylases (NADPME and PEPCK), transamination and partitioning of C4 metabolic processes between mesophyll and bundle sheath cells allows light capture to be balanced for the maize C4 pathway. Plant Physiology 164: 466-480

Pubmed: Author and Title
CrossRef: Author and Title
Google Scholar: Author Only Title Only Author and Title

Bellasio C, Lundgren MR (2016) Anatomical constraints to C4 evolution: light harvesting capacity in the bundle sheath. New Phytologist 212: 485-496

Pubmed: Author and Title
CrossRef: Author and Title
Google Scholar: Author Only Title Only Author and Title

Berry JA, Beerling DJ, Franks PJ (2010) Stomata: key players in the earth system, past and present. Current Opinion in Plant Biology 13: 232-239
Pubmed: Author and Title
CrossRef: Author and Title
Google Scholar: Author Only Title Only Author and Title

Berry JA, Farquhar GD (1978) The CO2 concentrating function of C4 photosynthesis: a biochemical model. In D Hall, J Coombs, T Goodwin, eds, Proceedings of the 4th International Congress on Photosynthesis. Biochemical Society, pp 119-131
Pubmed: Author and Title
CrossRef: Author and Title
Google Scholar: Author Only Title Only Author and Title

Boesgaard KS, Mikkelsen TN, Ro-Poulsen H, Ibrom A (2013) Reduction of molecular gas diffusion through gaskets in leaf gas exchange cuvettes by leaf-mediated pores. Plant, Cell & Environment 36: 1352-1362
Pubmed: Author and Title
CrossRef: Author and Title
Google Scholar: Author Only Title Only Author and Title

Bonan GB, Williams M, Fisher RA, Oleson KW (2014) Modeling stomatal conductance in the earth system: linking leaf water-use efficiency and water transport along the soil-plant-atmosphere continuum. Geosci. Model Dev. 7: 2193-2222
Pubmed: Author and Title
CrossRef: Author and Title
Google Scholar: Author Only Title Only Author and Title

Brodribb TJ, McAdam SAM (2017) Evolution of the Stomatal Regulation of Plant Water Content. Plant Physiology 174: 639-649
Pubmed: Author and Title
CrossRef: Author and Title
Google Scholar: Author Only Title Only Author and Title

Buckley TN (2005) The control of stomata by water balance. New Phytologist 168: 275-292
Pubmed: Author and Title
CrossRef: Author and Title
Google Scholar: Author Only Title Only Author and Title

Buckley TN (2017) Modeling stomatal conductance. Plant Physiology DOI:10.1104/pp.16.01772
Pubmed: Author and Title
CrossRef: Author and Title
Google Scholar: Author Only Title Only Author and Title

Buckley TN, Martorell S, Diaz-Espejo A, Tomas M, Medrano H (2014) Is stomatal conductance optimized over both time and space in plant crowns? A field test in grapevine (Vitis vinifera). Plant Cell and Environment 37: 2707-2721
Pubmed: Author and Title
CrossRef: Author and Title
Google Scholar: Author Only Title Only Author and Title

Buckley TN, Mott KA, Farquhar GD (2003) A hydromechanical and biochemical model of stomatal conductance. Plant, Cell & Environment 26: 1767-1785
Pubmed: Author and Title
CrossRef: Author and Title
Google Scholar: Author Only Title Only Author and Title

Buckley TN, Sack L, Farquhar GD (2016) Optimal plant water economy. Plant, Cell & Environment
Pubmed: Author and Title
CrossRef: Author and Title
Google Scholar: Author Only Title Only Author and Title

Buckley TN, Sack L, Gilbert ME (2011) The Role of Bundle Sheath Extensions and Life Form in Stomatal Responses to Leaf Water Status. Plant Physiology 156: 962-973
Pubmed: Author and Title
CrossRef: Author and Title
Google Scholar: Author Only Title Only Author and Title

Buckley TN, Schymanski SJ (2014) Stomatal optimisation in relation to atmospheric CO2. New Phytologist 201: 372-377
Pubmed: Author and Title
CrossRef: Author and Title
Google Scholar: Author Only Title Only Author and Title

Busch FA (2014) Opinion: The red-light response of stomatal movement is sensed by the redox state of the photosynthetic electron transport chain. Photosynthesis Research 119: 131-140
Pubmed: Author and Title
CrossRef: Author and Title
Google Scholar: Author Only Title Only Author and Title

Chen JW, Yang ZQ, Zhou P, Hai MR, Tang TX, Liang YL, An TX (2013) Biomass accumulation and partitioning, photosynthesis, and photosynthetic induction in field-grown maize (Zea mays L.) under low- and high-nitrogen conditions. Acta Physiologiae Plantarum 35: 95-105
Pubmed: Author and Title
CrossRef: Author and Title
Google Scholar: Author Only Title Only Author and Title

Cochard H, Venisse J-S, Barigah TS, Brunel N, Herbette S, Guilliot A, Tyree MT, Sakr S (2007) Putative Role of Aquaporins in

Variable Hydraulic Conductance of Leaves in Response to Light. Plant Physiology 143: 122-133
Pubmed: Author and Title
CrossRef: Author and Title
Google Scholar: Author Only Title Only Author and Title

Collatz GJ, Ribas-Carbo M, Berry JA (1992) Coupled Photosynthesis-Stomatal Conductance Model for Leaves of C4 Plants. Australian Journal of Plant Physiology 19: 519-538
Pubmed: Author and Title
CrossRef: Author and Title
Google Scholar: Author Only Title Only Author and Title

Cowan I, Farquhar G (1977) Stomatal function in relation to leaf metabolism and environment. In Symposia of the Society for Experimental Biology, Vol 31, p 471
Pubmed: Author and Title
CrossRef: Author and Title
Google Scholar: Author Only Title Only Author and Title

Cunniff J, Charles M, Jones G, Osborne CP (2016) Reduced plant water status under sub-ambient pCO2 limits plant productivity in the wild progenitors of C3 and C4 cereals. Annals of Botany 118: 1163-1173
Pubmed: Author and Title
CrossRef: Author and Title
Google Scholar: Author Only Title Only Author and Title

Damour G, Simonneau T, Cochard H, Urban L (2010) An overview of models of stomatal conductance at the leaf level. Plant, Cell & Environment 33: 1419-1438
Pubmed: Author and Title
CrossRef: Author and Title
Google Scholar: Author Only Title Only Author and Title

de Boer HJ, Lammertsma EI, Wagner-Cremer F, Dilcher DL, Wassen MJ, Dekker SC (2011) Climate forcing due to optimization of maximal leaf conductance in subtropical vegetation under rising CO2. Proceedings of the National Academy of Sciences 108: 4041-4046
Pubmed: Author and Title
CrossRef: Author and Title
Google Scholar: Author Only Title Only Author and Title

Diaz-Espejo A, Buckley TN, Sperry JS, Cuevas MV, de Cires A, Elsayed-Farag S, Martin-Palomo MJ, Muriel JL, Perez-Martin A, Rodriguez-Dominguez CM, Rubio-Casal AE, Torres-Ruiz JM, Fernandez JE (2012) Steps toward an improvement in process-based models of water use by fruit trees: A case study in olive. Agricultural Water Management 114: 37-49
Pubmed: Author and Title
CrossRef: Author and Title
Google Scholar: Author Only Title Only Author and Title

Ehleringer JR, Cerling TE, Helliker BR (1997) C4 photosynthesis, atmospheric CO2, and climate. Oecologia 112: 285-299
Pubmed: Author and Title
CrossRef: Author and Title
Google Scholar: Author Only Title Only Author and Title

FAO (2012) Fao Statistical division web page, Rome In, www.fao.org

Farquhar G, Wong S (1984) An empirical model of stomatal conductance. Functional Plant Biology 11: 191-210
Pubmed: Author and Title
CrossRef: Author and Title
Google Scholar: Author Only Title Only Author and Title

Fini A, Bellasio C, Pollastri S, Tattini M, Ferrini F (2013) Water relations, growth, and leaf gas exchange as affected by water stress in Jatropha curcas. Journal of Arid Environments 89: 21-29
Pubmed: Author and Title
CrossRef: Author and Title
Google Scholar: Author Only Title Only Author and Title

Foyer CH, Neukermans J, Queval G, Noctor G, Harbinson J (2012) Photosynthetic control of electron transport and the regulation of gene expression. Journal of Experimental Botany 63: 1637-1661
Pubmed: Author and Title
CrossRef: Author and Title
Google Scholar: Author Only Title Only Author and Title

Franks PJ, Cowan IR, Tyerman SD, Cleary AL, Lloyd J, Farquhar GD (1995) Guard-Cell Pressure Aperture Characteristics Measured with the Pressure Probe. Plant Cell and Environment 18: 795-800
Pubmed: Author and Title
CrossRef: Author and Title
Google Scholar: Author Only Title Only Author and Title

Franks PJ, Farquhar GD (2007) The mechanical diversity of stomata and its significance in gas-exchange control. Plant Physiology 143: 78-87
Pubmed: Author and Title
CrossRef: Author and Title
Google Scholar: Author Only Title Only Author and Title

Franks PJ, Leitch IJ, Ruszala EM, Hetherington AM, Beerling DJ (2012) Physiological framework for adaptation of stomata to CO2 from glacial to future concentrations. Philosophical Transactions of the Royal Society B-Biological Sciences 367: 537-546

Pubmed: Author and Title
CrossRef: Author and Title
Google Scholar: Author Only Title Only Author and Title

Ghannoum O (2009) C4 photosynthesis and water stress. Annals of Botany 103: 635-644
Pubmed: Author and Title
CrossRef: Author and Title
Google Scholar: Author Only Title Only Author and Title

Ghannoum O, Caemmerer SV, Ziska LH, Conroy JP (2000) The growth response of C4 plants to rising atmospheric CO2 partial pressure: a reassessment. Plant, Cell & Environment 23: 931-942
Pubmed: Author and Title
CrossRef: Author and Title
Google Scholar: Author Only Title Only Author and Title

Ghannoum O, Conroy JP, Driscoll SP, Paul MJ, Foyer CH, Lawlor DW (2003) Nonstomatal limitations are responsible for drought-induced photosynthetic inhibition in four C4 grasses. New Phytologist 159: 599-608
Pubmed: Author and Title
CrossRef: Author and Title
Google Scholar: Author Only Title Only Author and Title

Givnish TJ, Vermeij GJ (1976) Sizes and Shapes of Liane Leaves. American Naturalist 110: 743-778
Pubmed: Author and Title
CrossRef: Author and Title
Google Scholar: Author Only Title Only Author and Title

Griffiths H, Weller G, Toy LFM, Dennis RJ (2013) You're so vein: bundle sheath physiology, phylogeny and evolution in C3 and C4 plants. Plant, Cell & Environment 36: 249-261
Pubmed: Author and Title
CrossRef: Author and Title
Google Scholar: Author Only Title Only Author and Title

Gross LJ, Kirschbaum MUF, Pearcy RW (1991) A Dynamic-Model of Photosynthesis in Varying Light Taking Account of Stomatal Conductance, C3-Cycle Intermediates, Photorespiration and Rubisco Activation. Plant Cell and Environment 14: 881-893
Pubmed: Author and Title
CrossRef: Author and Title
Google Scholar: Author Only Title Only Author and Title

Horrer D, Flutsch S, Pazmino D, Matthews JSA, Thalmann M, Nigro A, Leonhardt N, Lawson T, Santelia D (2016) Blue Light Induces a Distinct Starch Degradation Pathway in Guard Cells for Stomatal Opening. Current Biology 26: 362-370
Pubmed: Author and Title
CrossRef: Author and Title
Google Scholar: Author Only Title Only Author and Title

Jarvis PG (1976) The interpretation of the variations in leaf water potential and stomatal conductance found in canopies in the field. Philosophical Transactions of the Royal Society of London. B, Biological Sciences 273: 593-610
Pubmed: Author and Title
CrossRef: Author and Title
Google Scholar: Author Only Title Only Author and Title

Kim YX, Steudle E (2007) Light and turgor affect the water permeability (aquaporins) of parenchyma cells in the midrib of leaves of Zea mays. Journal of Experimental Botany 58: 4119-4129
Pubmed: Author and Title
CrossRef: Author and Title
Google Scholar: Author Only Title Only Author and Title

Knapp AK (1993) Gas-Exchange Dynamics in C3 and C4 Grasses - Consequences of Differences in Stomatal Conductance. Ecology 74: 113-123
Pubmed: Author and Title
CrossRef: Author and Title
Google Scholar: Author Only Title Only Author and Title

Kramer DM, Avenson TJ, Edwards GE (2004) Dynamic flexibility in the light reactions of photosynthesis governed by both electron and proton transfer reactions. Trends in Plant Science 9: 349-357
Pubmed: Author and Title
CrossRef: Author and Title
Google Scholar: Author Only Title Only Author and Title

Lawson T, Blatt MR (2014) Stomatal Size, Speed, and Responsiveness Impact on Photosynthesis and Water Use Efficiency. Plant Physiology 164: 1556-1570
Pubmed: Author and Title
CrossRef: Author and Title
Google Scholar: Author Only Title Only Author and Title

Leuning R (1995) A critical appraisal of a combined stomatal-photosynthesis model for C3 plants. Plant, Cell & Environment 18: 339-355
Pubmed: Author and Title
CrossRef: Author and Title
Google Scholar: Author Only Title Only Author and Title

Manzoni S, Vico G, Palmroth S, Porporato A, Katul G (2013) Optimization of stomatal conductance for maximum carbon gain under

dynamic soil moisture. Advances in Water Resources 62, Part A: 90-105
Pubmed: Author and Title
CrossRef: Author and Title
Google Scholar: Author Only Title Only Author and Title

McAusland L, Vialet-Chabrand S, Davey P, Baker NR, Brendel O, Lawson T (2016) Effects of kinetics of light-induced stomatal responses on photosynthesis and water-use efficiency. New Phytologist 211: 1209-1220
Pubmed: Author and Title
CrossRef: Author and Title
Google Scholar: Author Only Title Only Author and Title

Messinger SM, Buckley TN, Mott KA (2006) Evidence for involvement of photosynthetic processes in the stomatal response to CO2. Plant Physiology 140: 771-778
Pubmed: Author and Title
CrossRef: Author and Title
Google Scholar: Author Only Title Only Author and Title

Morison JI, Gifford RM (1983) Stomatal Sensitivity to Carbon Dioxide and Humidity a comparison of two C3 and two C4 grass species. Plant Physiology 71: 789-796
Pubmed: Author and Title
CrossRef: Author and Title
Google Scholar: Author Only Title Only Author and Title

Mott KA, Berg DG, Hunt SM, Peak D (2014) Is the signal from the mesophyll to the guard cells a vapour-phase ion? Plant Cell and Environment 37: 1184-1191
Pubmed: Author and Title
CrossRef: Author and Title
Google Scholar: Author Only Title Only Author and Title

Osborne CP, Sack L (2012) Evolution of C4 plants: a new hypothesis for an interaction of CO2 and water relations mediated by plant hydraulics. Philosophical Transactions of the Royal Society B-Biological Sciences 367: 583-600
Pubmed: Author and Title
CrossRef: Author and Title
Google Scholar: Author Only Title Only Author and Title

Ostle NJ, Smith P, Fisher R, Ian Woodward F, Fisher JB, Smith JU, Galbraith D, Levy P, Meir P, McNamara NP, Bardgett RD (2009) Integrating plant-soil interactions into global carbon cycle models. Journal of Ecology 97: 851-863
Pubmed: Author and Title
CrossRef: Author and Title
Google Scholar: Author Only Title Only Author and Title

Paschalis A, Katul GG, Fatichi S, Palmroth S, Way D (2017) On the variability of the ecosystem response to elevated atmospheric CO2 across spatial and temporal scales at the Duke Forest FACE experiment. Agricultural and Forest Meteorology 232: 367-383
Pubmed: Author and Title
CrossRef: Author and Title
Google Scholar: Author Only Title Only Author and Title

Pearcy RW, Gross LJ, He D (1997) An improved dynamic model of photosynthesis for estimation of carbon gain in sunfleck light regimes. Plant Cell and Environment 20: 411-424
Pubmed: Author and Title
CrossRef: Author and Title
Google Scholar: Author Only Title Only Author and Title

Pinto H, Sharwood RE, Tissue DT, Ghannoum O (2014) Photosynthesis of C3, C3-C4, and C4 grasses at glacial CO2. Journal of Experimental Botany 65: 3669-3681
Pubmed: Author and Title
CrossRef: Author and Title
Google Scholar: Author Only Title Only Author and Title

Raven JA (2002) Selection pressures on stomatal evolution. New Phytologist 153: 371-386
Pubmed: Author and Title
CrossRef: Author and Title
Google Scholar: Author Only Title Only Author and Title

Rodriguez-Dominguez CM, Buckley TN, Egea G, de Cires A, Hernandez-Santana V, Martorell S, Diaz-Espejo A (2016) Most stomatal closure in woody species under moderate drought can be explained by stomatal responses to leaf turgor. Plant, Cell & Environment 39: 2014-2026
Pubmed: Author and Title
CrossRef: Author and Title
Google Scholar: Author Only Title Only Author and Title

Sack L, Holbrook NM (2006) Leaf hydraulics. Annu Rev Plant Biol 57: 361-381
Pubmed: Author and Title
CrossRef: Author and Title
Google Scholar: Author Only Title Only Author and Title

Sage RF (2014) Stopping the leaks: New insights into C4 photosynthesis at low light. Plant, Cell & Environment 37: 1037-1041
Pubmed: Author and Title
CrossRef: Author and Title
Google Scholar: Author Only Title Only Author and Title

Sato H, Kumagai To, Takahashi A, Katul GG (2015) Effects of different representations of stomatal conductance response to humidity across the African continent under warmer CO2-enriched climate conditions. Journal of Geophysical Research: Biogeosciences 120: 979-988
Pubmed: Author and Title
CrossRef: Author and Title
Google Scholar: Author Only Title Only Author and Title

Sharkey TD, Raschke K (1981) Separation and Measurement of Direct and Indirect Effects of Light on Stomata. Plant Physiology 68: 33-40
Pubmed: Author and Title
CrossRef: Author and Title
Google Scholar: Author Only Title Only Author and Title

Sharp RE, Davies WJ (1979) Solute regulation and growth by roots and shoots of water-stressed maize plants. Planta 147: 43-49
Pubmed: Author and Title
CrossRef: Author and Title
Google Scholar: Author Only Title Only Author and Title

Shimazaki K, Iino M, Zeiger E (1986) Blue light-dependent proton extrusion by guard-cell protoplasts of Vicia faba. Nature 319: 324-326
Pubmed: Author and Title
CrossRef: Author and Title
Google Scholar: Author Only Title Only Author and Title

Stitt M, Zhu X-G (2014) The large pools of metabolites involved in intercellular metabolite shuttles in C4 photosynthesis provide enormous flexibility and robustness in a fluctuating light environment. Plant, Cell & Environment 37: 1985-1988
Pubmed: Author and Title
CrossRef: Author and Title
Google Scholar: Author Only Title Only Author and Title

Taylor SH, Hulme SP, Rees M, Ripley BS, Ian Woodward F, Osborne CP (2010) Ecophysiological traits in C3 and C4 grasses: a phylogenetically controlled screening experiment. New Phytologist 185: 780-791
Pubmed: Author and Title
CrossRef: Author and Title
Google Scholar: Author Only Title Only Author and Title

Taylor SH, Ripley BS, Woodward FI, Osborne CP (2011) Drought limitation of photosynthesis differs between C3 and C4 grass species in a comparative experiment. Plant, Cell & Environment 34: 65-75
Pubmed: Author and Title
CrossRef: Author and Title
Google Scholar: Author Only Title Only Author and Title

Ubierna N, Gandin A, Boyd RA, Cousins AB (2016) Temperature response of mesophyll conductance in three C4 species calculated with two methods: 18O discrimination and in vitro Vpmax. New Phytologist 214: 66-80
Pubmed: Author and Title
CrossRef: Author and Title
Google Scholar: Author Only Title Only Author and Title

Vialet-Chabrand S, Matthews JSA, Brendel O, Blatt MR, Wang Y, Hills A, Griffiths H, Rogers S, Lawson T (2016) Modelling water use efficiency in a dynamic environment: An example using Arabidopsis thaliana. Plant Science 251: 65-74
Pubmed: Author and Title
CrossRef: Author and Title
Google Scholar: Author Only Title Only Author and Title

Volder A, Tjoelker MG, Briske DD (2010) Contrasting physiological responsiveness of establishing trees and a C4 grass to rainfall events, intensified summer drought, and warming in oak savanna. Global Change Biology 16: 3349-3362
Pubmed: Author and Title
CrossRef: Author and Title
Google Scholar: Author Only Title Only Author and Title

von Caemmerer S (2000) Biochemical models of leaf Photosynthesis. CSIRO Publishing, Collingwood
Pubmed: Author and Title
CrossRef: Author and Title
Google Scholar: Author Only Title Only Author and Title

Wand SJE, Midgley GF, Jones MH, Curtis PS (1999) Responses of wild C4 and C3 grass (Poaceae) species to elevated atmospheric CO2 concentration: a meta-analytic test of current theories and perceptions. Global Change Biology 5: 723-741
Pubmed: Author and Title
CrossRef: Author and Title
Google Scholar: Author Only Title Only Author and Title

Wand SJE, Midgley GF, Stock WD (2001) Growth responses to elevated CO2 in NADP-ME, NAD-ME and PCK C4 grasses and a C3 grass from South Africa. Functional Plant Biology 28: 13-25
Pubmed: Author and Title
CrossRef: Author and Title
Google Scholar: Author Only Title Only Author and Title

Ward JK, Tissue DT, Thomas RB, Strain BR (1999) Comparative responses of model C3 and C4 plants to drought in low and elevated CO2. Global Change Biology 5: 857-867
Pubmed: Author and Title

CrossRef: Author and Title
Google Scholar: Author Only Title Only Author and Title

Way DA, Oren R, Kim HS, Katul GG (2011) How well do stomatal conductance models perform on closing plant carbon budgets? A test using seedlings grown under current and elevated air temperatures. Journal of Geophysical Research: Biogeosciences (2005-2012) 116

Pubmed: Author and Title
CrossRef: Author and Title
Google Scholar: Author Only Title Only Author and Title

Wong SC (1979) Elevated atmospheric partial-pressure of CO2 and plant-growth .1. Interactions of nitrogen nutrition and photosynthetic capacity in C3 and C4 plants. Oecologia 44: 68-74

Pubmed: Author and Title
CrossRef: Author and Title
Google Scholar: Author Only Title Only Author and Title

Yin X, Struik PC (2009) C3 and C4 photosynthesis models: An overview from the perspective of crop modelling. Njas-Wageningen Journal of Life Sciences 57: 27-38

Pubmed: Author and Title
CrossRef: Author and Title
Google Scholar: Author Only Title Only Author and Title

Yin X, Struik PC (2015) Constraints to the potential efficiency of converting solar radiation into phytoenergy in annual crops: from leaf biochemistry to canopy physiology and crop ecology. Journal of Experimental Botany 66: 6535-6549

Pubmed: Author and Title
CrossRef: Author and Title
Google Scholar: Author Only Title Only Author and Title